

**A novel (3,3,6)-connected luminescent metal-organic framework for sensing of
nitroaromatic explosives**

Libo Sun,^a Hongzhu Xing,^b Jin Xu,^a Zhiqiang Liang,*^a Jihong Yu,^a Ruren Xu^a

^aState Key Laboratory of Inorganic Synthesis and Preparative Chemistry, College of chemistry, Jilin University, Changchun 130012, China

^bCollege of Chemistry, Northeast Normal University, Changchun, P. R. China.

E-mail: liangzq@jlu.edu.cn

Fax: +86-431-85168609

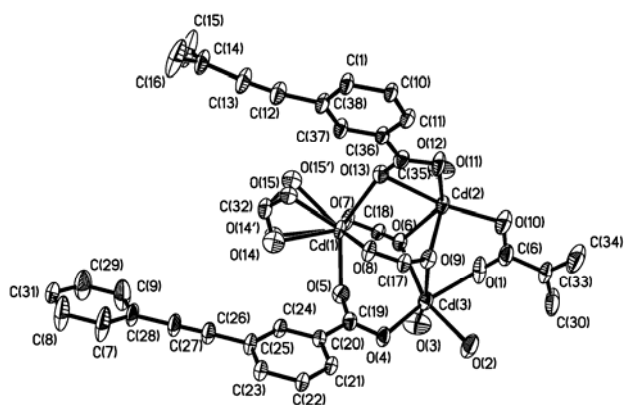


Fig. S1 Representation of the asymmetric unit of **1** showing ellipsoid at the 30% probability level. The hydrogen atoms and coordinated DMF molecules are omitted for clarity.

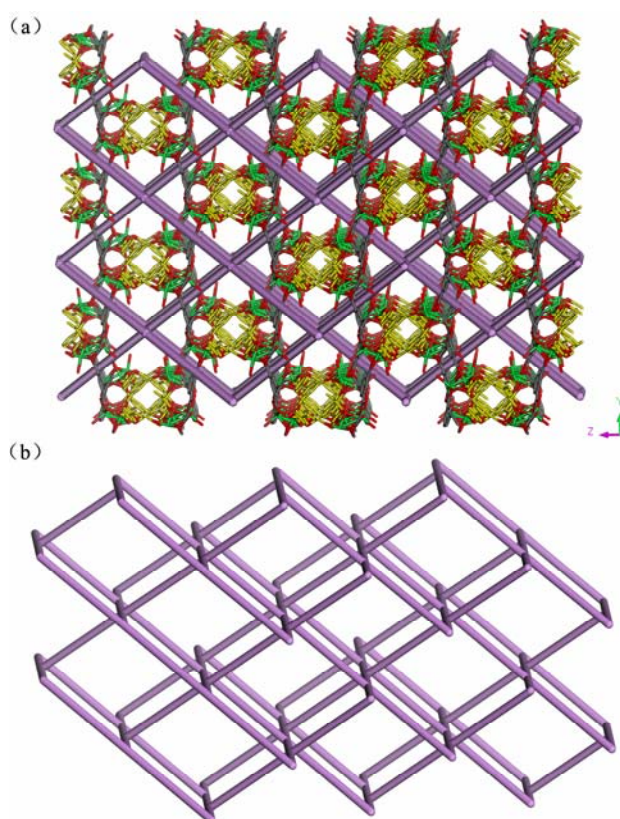


Fig. S2 (a) The representation of 3D channels along the $[1\ 0\ 1]$, $[1\ 1\ 0]$ and $[-1\ 1\ 0]$ direction; (b) Schematic representation of the cross-linked 3D channels. The hydrogen atoms and coordinated DMF molecules are omitted for clarity.

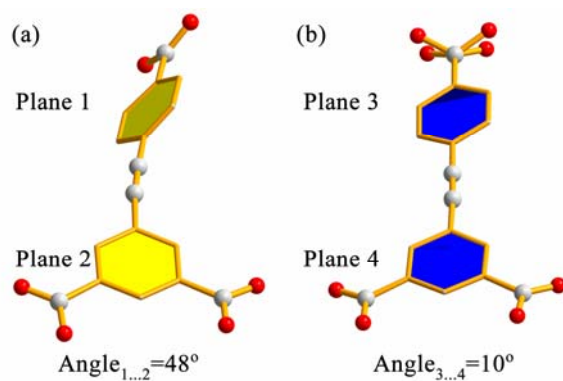


Fig. S3 Comparison of the dihedral angle between the two planes of ligand L and L', respectively: (a) the dihedral angle of ligand L; (b) the dihedral angle of ligand L'.

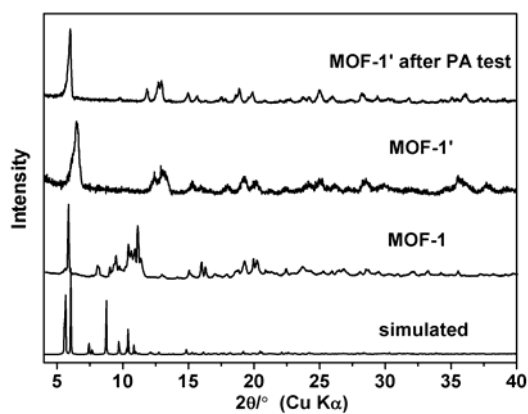


Fig. S4 Powder X-ray diffraction patterns comparison of **1**, **1'** and **1'** after PA test.

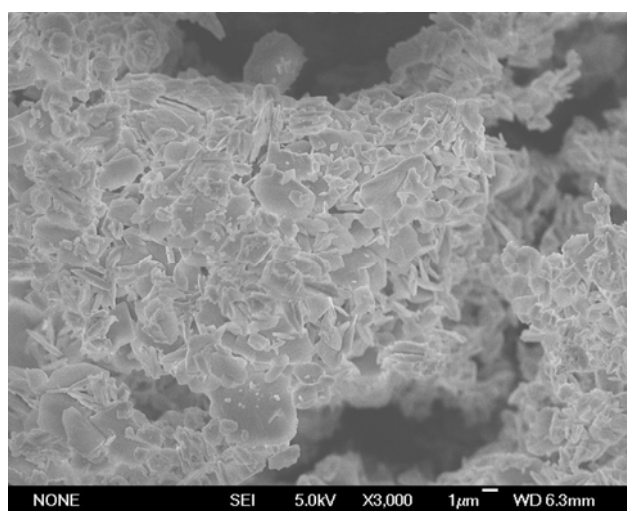


Fig. S5 Scanning electron microscope image for **1'**

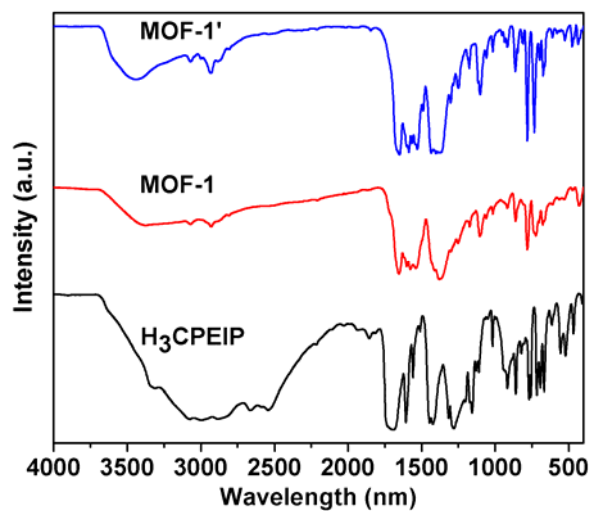


Fig. S6 FT-IR spectra of **1** and **1'**.

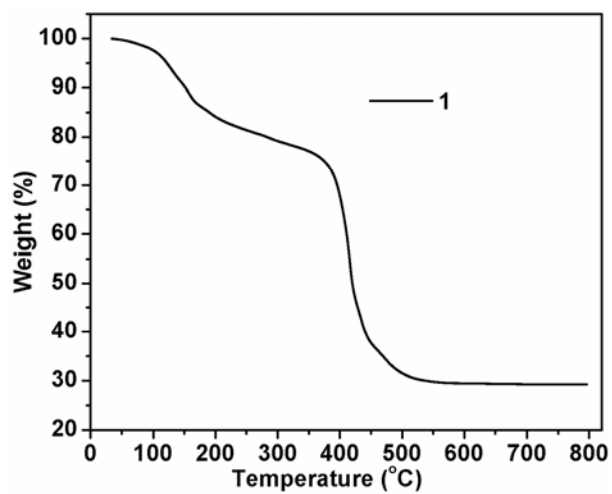


Fig. S7 TGA curve for **1**

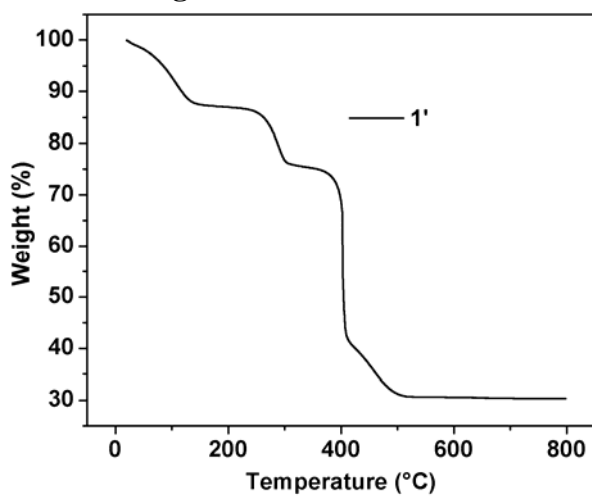


Fig. S8 TGA curve for **1'**.

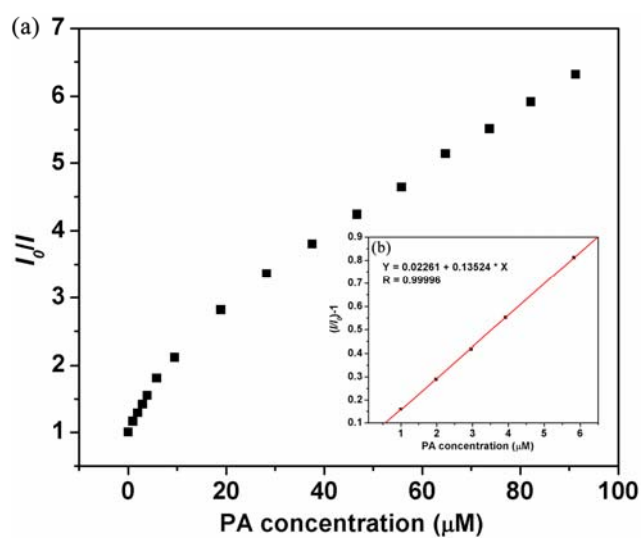


Fig. S9 Plot of I_0/I versus PA concentration in ethanol for **1'**.

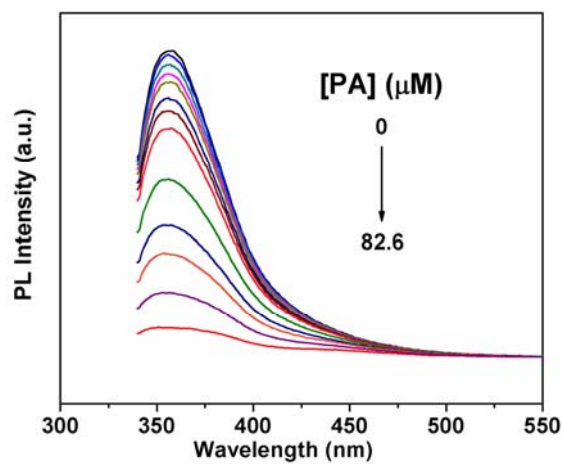


Fig. S10 Fluorescent quenching of the ligand H_3CPEIP dissolved in ethanol solution by gradual addition of PA.

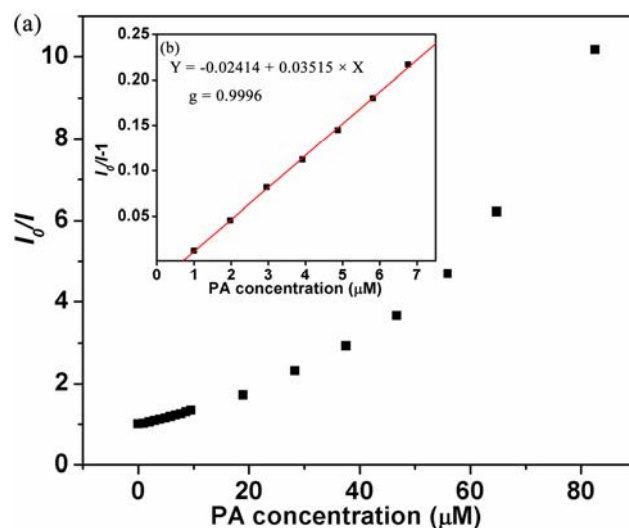


Fig. S11 Plot of I_0/I versus PA concentration in ethanol for H_3CPEIP .

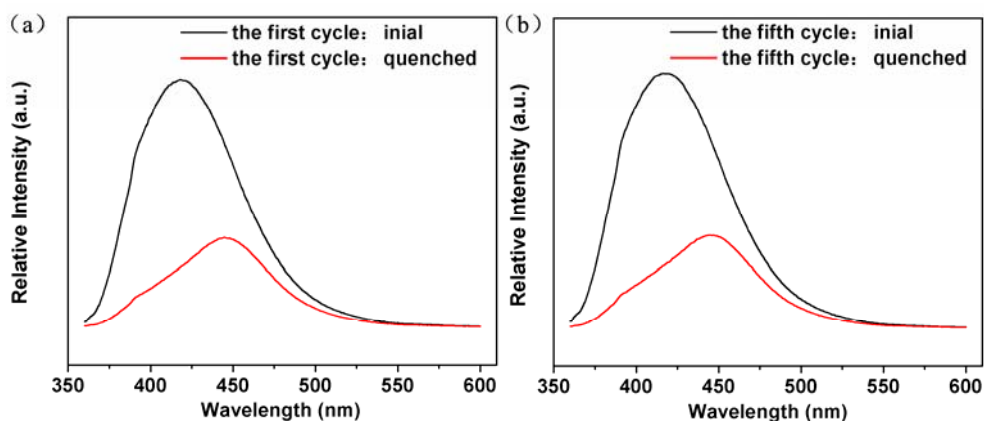


Fig. S12 Comparison of the first and the fifth cyclic for PA quenching experiments.

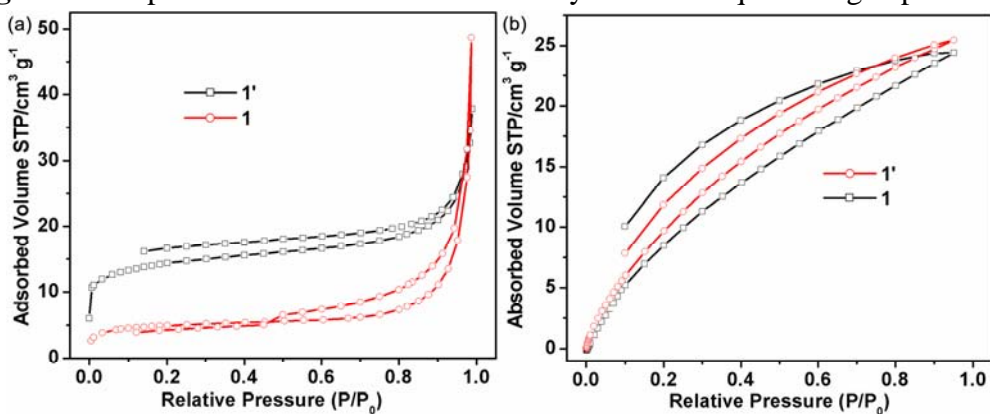


Fig. S13 (a) N_2 adsorption-desorption isotherms measured at 77 K. (b) CO_2 adsorption-desorption isotherms measured at 273 K.

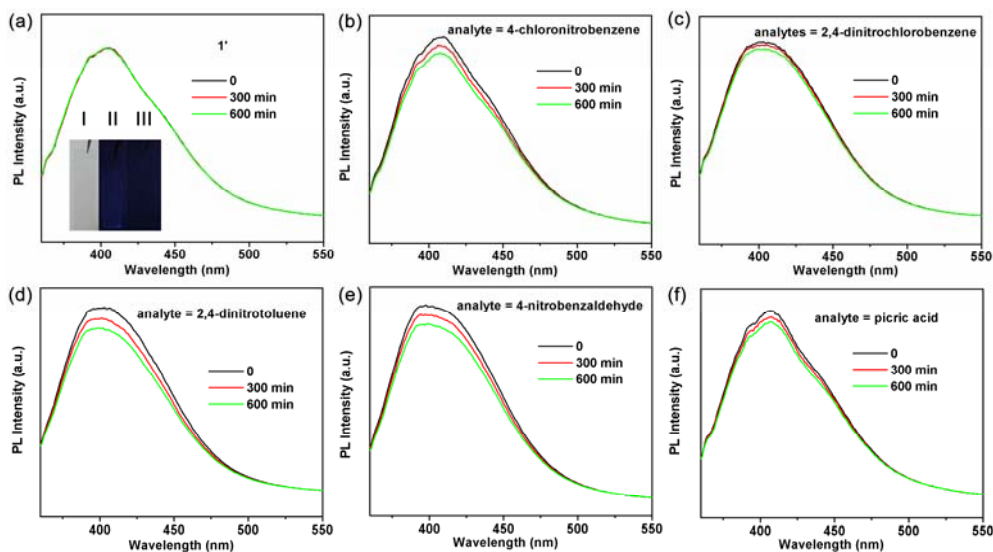


Fig. S14 The vapor sensing experiments. The small photos in (a) represents: I, the **1'**@PMMA in the sunlight; II, the **1'**@PMMA in the UV light; III, the PMMA in the UV light (365 nm).

Table S1. Selected bond distances (Å) and angles (°) for compound **1**.

Bond distances/ Å

Cd(1)-O(15)	2.279(8)
Cd(1)-O(8)	2.300(3)
Cd(1)-O(7)	2.343(4)
Cd(1)-O(5)	2.345(4)
Cd(1)-O(14)	2.346(12)
Cd(1)-O(15')	2.382(9)
Cd(1)-O(13)	2.397(4)
Cd(1)-O(14')	2.464(9)
Cd(2)-O(10)	2.191(4)
Cd(2)-O(11)	2.223(5)
Cd(2)-O(12)	2.230(4)
Cd(2)-O(6)	2.301(4)
Cd(2)-O(9)	2.361(3)
Cd(2)-O(13)	2.526(3)
Cd(3)-O(4)	2.217(4)
Cd(3)-O(3)	2.220(6)
Cd(3)-O(1)	2.294(5)
Cd(3)-O(2)	2.298(4)
Cd(3)-O(9)	2.341(4)
Cd(3)-O(6)	2.414(3)

Bond angles/ °

O(15)-Cd(1)-O(8)	98.0(2)
O(15)-Cd(1)-O(7)	114.2(2)
O(8)-Cd(1)-O(7)	146.40(11)
O(15)-Cd(1)-O(5)	125.5(2)
O(8)-Cd(1)-O(5)	81.55(14)
O(7)-Cd(1)-O(5)	87.09(14)
O(15)-Cd(1)-O(14)	47.6(4)
O(8)-Cd(1)-O(14)	108.7(3)
O(7)-Cd(1)-O(14)	100.4(3)
O(5)-Cd(1)-O(14)	80.6(3)
O(15)-Cd(1)-O(15')	20.0(3)
O(8)-Cd(1)-O(15')	114.0(3)
O(7)-Cd(1)-O(15')	95.9(3)
O(5)-Cd(1)-O(15')	136.6(3)
O(14)-Cd(1)-O(15')	56.2(4)
O(15)-Cd(1)-O(13)	88.7(2)
O(8)-Cd(1)-O(13)	80.38(13)
O(7)-Cd(1)-O(13)	90.57(14)
O(5)-Cd(1)-O(13)	143.25(12)
O(14)-Cd(1)-O(13)	135.6(3)
O(15')-Cd(1)-O(13)	80.1(2)
O(15)-Cd(1)-O(14')	55.0(3)
O(8)-Cd(1)-O(14')	127.9(2)
O(7)-Cd(1)-O(14')	81.1(2)
O(5)-Cd(1)-O(14')	82.4(2)
O(14)-Cd(1)-O(14')	19.5(3)
O(15')-Cd(1)-O(14')	55.6(3)
O(13)-Cd(1)-O(14')	133.4(2)
O(10)-Cd(2)-O(11)	103.4(2)
O(10)-Cd(2)-O(12)	100.1(2)
O(11)-Cd(2)-O(12)	106.78(19)
O(10)-Cd(2)-O(6)	120.69(19)
O(11)-Cd(2)-O(6)	85.91(18)
O(12)-Cd(2)-O(6)	133.44(13)
O(10)-Cd(2)-O(9)	86.61(18)
O(11)-Cd(2)-O(9)	158.54(18)
O(12)-Cd(2)-O(9)	89.71(16)
O(6)-Cd(2)-O(9)	72.70(12)
O(10)-Cd(2)-O(13)	153.9(2)
O(11)-Cd(2)-O(13)	91.56(19)
O(12)-Cd(2)-O(13)	54.56(12)
O(6)-Cd(2)-O(13)	81.15(12)
O(9)-Cd(2)-O(13)	86.91(12)

O(4)-Cd(3)-O(3)	99.2(2)
O(4)-Cd(3)-O(1)	161.15(16)
O(3)-Cd(3)-O(1)	94.7(2)
O(4)-Cd(3)-O(2)	83.31(16)
O(3)-Cd(3)-O(2)	98.5(2)
O(1)-Cd(3)-O(2)	82.01(17)
O(4)-Cd(3)-O(9)	88.29(14)
O(3)-Cd(3)-O(9)	163.77(18)
O(1)-Cd(3)-O(9)	81.76(17)
O(2)-Cd(3)-O(9)	96.64(17)
O(4)-Cd(3)-O(6)	112.28(12)
O(3)-Cd(3)-O(6)	92.78(18)
O(1)-Cd(3)-O(6)	79.58(14)
O(2)-Cd(3)-O(6)	159.10(17)
O(9)-Cd(3)-O(6)	71.03(11)
